

Dust Extinction towards the Type Ia Supernova 2012cu in NGC 4772

WEIJIA GAO^a, RUINING ZHAO^a, JIAN GAO^{a,*}, BIWEI JIANG^a, JUN
LI^a

^a*Department of astronomy, Beijing Normal University, Beijing 100875, China*

Abstract

Using photometric and spectroscopic data of Supernova (SN) 2012cu, a fairly reddened type Ia supernova, we derived its color excess curves and probed the dust extinction in its host galaxy, NGC 4772. In order to derive the extinction as a function of wavelength (i.e., A_λ), we model the color excess curves of SN 2012cu in terms of dust models consisting of silicate and carbonaceous (graphite or amorphous carbon) dust. The modeled extinction law towards SN 2012cu extends flatly to the far-ultraviolet (UV) bands, which is much flatter than those of the Milky Way and Magellanic Clouds, and the 2175Å feature is very weak or absent. The flatness of the modeled extinction curve in the UV bands suggests a “grey” extinction law of the active galactic nucleus in the vicinity of the SN 2012cu-Earth line of sight. Our results indicate that the sizes of the dust in the ISM towards SN 2012cu in NGC 4772 are larger than those of the Milky Way and the Large Magellanic Cloud, and much larger than that of the Small Magellanic Cloud. The best fitting gives an observed visual extinction towards SN 2012cu of $A_V \approx 2.6$ mag, a reddening

*Corresponding author

Email address: jiangao@bnu.edu.cn (JIAN GAO)

of $E(B - V) \approx 1.0$ mag, with a total-to-selective extinction ratio $R_V \approx 2.7$, consistent with previous results.

Keywords: (ISM:) dust, extinction – galaxies: ISM – galaxies: individual (NGC 4772) – supernovae: individual (SN 2012cu)

1. Introduction

Attributed to their high luminosity with small dispersion at the maximum of light curves, type Ia supernovae (SNe Ia) are one of the most powerful “standard candles” for measuring cosmological distances (Riess et al. 1998, 2016; Perlmutter et al. 1999), leading to the discovery of accelerating universe and hence the presence of mysterious dark energy. Incomprehensive knowledge on the extinction towards SNe Ia will, however, result in a systematic uncertainty in the intrinsic luminosity and distances to SNe Ia, which leads to one of the major issues in SNe Ia cosmology as the correction for the line-of-sight extinction. In addition, due to the undetectable extragalactic environment, SNe Ia are often the only approach to study the extinction of extragalactic dust.

The wavelength dependence of the interstellar extinction [known as the “interstellar extinction law (or curve)”] is defined as A_λ at wavelength λ . Since A_λ is hard to obtain directly, astronomers often measure the color excesses $E(\lambda - V) \equiv A_\lambda - A_V$, where A_V is the extinction in the visual band. The color excesses of SNe Ia are often determined by comparing spectrophotometry of two sources with the same spectral shape, one of which has minor foreground reddening (i.e., Amanullah et al. 2014, 2015). The total-to-selective extinction ratio $R_V \equiv A_V / E(B - V)$ provides an adequate description of

the extinction laws of the Milky Way (MW) dust (e.g., [Cardelli et al. 1989](#), hereafter [CCM89](#); [Fitzpatrick 1999](#), hereafter [F99](#)), in which R_V ranges from 2.2 to 5.5 with the average value of 3.1 (e.g., [Fitzpatrick & Massa 2007](#)). However, [CCM89](#) and [F99](#) are not necessarily valid for the extinction laws for external galaxies, even for the Large and Small Magellanic Clouds (LMC, SMC; [Gordon et al. 2003](#)).

There is increasing evidence that extinction curves towards SNe Ia systematically favor a steeper law ($R_V < 3$, see, for instance, [Nobili & Goobar 2008](#); [Folatelli et al. 2010](#); [Cikota et al. 2016](#)) compared to the Galactic average value ($R_V = 3.1$, see [CCM89](#) or [F99](#)). This suggests the properties of extragalactic dust may be incompatible with the Milky Way dust. Additionally, scattering by circumstellar dust also tends to reduce R_V in the optical band ([Wang 2005](#); [Patat et al. 2007](#); [Goobar 2008](#)). This discrepancy leads to another one of the major issues in SNe Ia cosmology, which is to understand whether the systematically low R_V values towards SNe Ia are caused by 1) systematic differences from the optical properties of extragalactic dust grains, or 2) modifications by the circumstellar matter scattering.

In our previous work, [Gao et al. \(2015\)](#) found that the peculiar extinction law in the sightline of SN 2014J, one SN Ia with $R_V < 2$ (e.g., $R_V = 1.6 \pm 0.2$, [Foley et al. 2014](#)), cannot be explained by [CCM89](#). For comparison, the dust models of a mixture of silicate and graphite/amorphous carbon dust grains provide an excellent fitting to the observed color excess curves towards SN 2014J. The reddening curve fitting around the peak luminosity of SN 2014J gives $R_V \sim 1.7$ towards the SN 2014J line of sight, which is also generally consistent with many other studies ([Amanullah et al. 2014](#); [Foley et al. 2014](#);

Goobar et al. 2014; Brown et al. 2015; Yang et al. 2017).

SN 2012cu was first discovered on June 11.2 UT, 2012 by Itagaki et al. (2012) and later classified as a SN Ia on June 15 UT, 2012 by Marion et al. (2012). It locates at $(\alpha_{2000}, \delta_{2000}) = (12:53:29.35, +02:09:39.0)$, $3''.1$ east and $27''.1$ south of the nucleus of the host galaxy NGC 4772 at a distance of 15.6 ± 1.0 Mpc¹, which can be found in the Extragalactic Distance Database (EDD, Tully et al. 2009)². The host galaxy is a Sa-type spiral galaxy according to its morphology (Haynes et al. 2000), and also classified as a low-luminosity “dwarf” Seyfert nuclei (or low-ionization nuclear emission-line region, LINER) according to its spectral lines (Ho et al. 1997). SN 2012cu is regarded as one of the reddest SNe Ia with $E(B - V) \sim 1$ mag. In the previous studies, Amanullah et al. (2015, hereafter A15) derived $E(B - V) = 0.99 \pm 0.03$ mag and $R_V = 2.8 \pm 0.1$ of SN 2012cu by fitting its UV-to-near-infrared (NIR) photometric colors. Huang et al. (2017, hereafter H17) found their best-fit $E(B - V) = 1.00 \pm 0.03$ mag and $R_V = 2.95 \pm 0.08$ by dereddening its optical spectra at different epochs. Both A15 and H17 obtained the R_V values of SN 2012cu by using the R_V -based formula of F99.

In this work, using the photometric data from A15 and spectroscopic data from H17 (see §2), we measure the color excesses $E(\lambda - V)$ of SN 2012cu.

¹The measured distances to NGC 4772 show the discrepancy among previous studies. Amanullah et al. (2015) adopted a distance of 41 ± 9 Mpc derived from the distance modulus of 33.06 ± 0.36 mag for NGC 4772 (see Tully et al. 2008 and Table 1 therein), while Huang et al. (2017) obtained the distance modulus of 31.11 ± 0.15 mag corresponding to a distance of 16.6 ± 1.1 Mpc. Huang et al. (2017) thought that the former measured with Tully-Fisher relation would be too large due to the bulk of the gas in NGC 4772.

²<http://edd.ifa.hawaii.edu/>

Without making a priori assumption of any template extinction law, we derive R_V and A_λ of SN 2012cu from the far-UV to NIR bands, in terms of mixed dust models of silicate and graphite or amorphous carbon (see §3). The results are presented in §4, discussed in §5, and summarized in §6.

2. Observational Data

We utilize the photometric data of SN 2012cu published by A15³. Their observations were performed with *Hubble Space Telescope (HST)*/Wide-Field Camera 3 (WFC3) through passbands of $F225W$, $F275W$ and $F336W$; and Nordic Optical Telescope (NOT, Djupvik & Andersen 2010) /Andalucia Faint Object Spectrograph and Camera (AL-FOSC) in U , B , V , R and i , and NOTCam in the J , H and Ks bands. The wavelength of the observed spectral energy distribution (SED) ranges from 2346 to 21295Å (i.e., from the UV to NIR bands), and uncertainties range from 0.08 to 0.3 mag (e.g., ~ 0.08 mag for R filter, ~ 0.2 mag for Ks band and ~ 0.3 mag for $F225W$ and $F275W$ passbands, A15). In total, 31 measurements are collected at eight epochs⁴ (see A15 and Figure 6 therein). The colors of SN 2012cu are obtained by making the redshift corrections (K-corrections, e.g., Hamuy et al. 1993) and magnitude corrections (S-corrections, e.g., Stritzinger et al. 2002), and subtracting the MW foreground extinctions (A^{MW}) with the following equation (A15)

$$X - V = (m_X - A_X^{\text{MW}} - K_X) - (m_V - A_V^{\text{MW}} - K_V), \quad (1)$$

³All data and figures presented by A15 are available at <http://snova.fysik.su.se/dust/>.

⁴The epoch is the day relative to the B -band maximum light of the observation.

where X (V) is the rest-frame magnitude in the filter X (V); m_X and m_V are the observed magnitudes; K_X is the combined K and S corrections; A^{MW} and K_X are given by A15, who adopted the values of Schlafly & Finkbeiner (2011). Then the color excesses of SN 2012cu can be derived by using the following equation

$$E(X - V) = (X - V) - (X - V)_0, \quad (2)$$

where $(X - V)_0$ is the intrinsic color of the unreddened objects listed by A15, who combined the spectroscopic data of SN 2011fe and created a series of daily sampled unreddened SED templates to derive the intrinsic colors of SNe Ia. It will be described later in this section.

The spectroscopic data of SN 2012cu are taken from H17⁵ (see Figure 13 therein), which span 17 epochs from -6.8 days to 46.2 days. In this work, we use the spectra which span 15 epochs from -6.8 days to 31.2 days⁶. The spectra of SN 2012cu cover a wavelength range from 3300 to 9200Å, and have already been flux calibrated (Buton et al. 2013), host-galaxy subtracted and corrected for the MW foreground extinctions (Schlafly & Finkbeiner 2011).

In order to determine the intrinsic colors of SN 2012cu, we use the SED templates of SN 2011fe privately provided by Amanullah R. (A15). SN 2011fe, one of the best studied SNe Ia, is the rare one with high-quality UV time series spectra obtained with *HST* (Foley et al. 2014; Mazzali et al. 2014). Furthermore, the extremely low host reddening (i.e., $E(B - V)_{\text{host}} =$

⁵The spectra of SN 2012cu are available at <http://snfactory.lbl.gov/TBD>.

⁶The epochs at 41.2 and 46.2 days are excluded because the SED templates of SN 2011fe used in this work only extend to 40 days past B -band maximum (see A15 and APPENDIX B therein).

0.026 ± 0.036 mag, Nugent et al. 2011; Pereira et al. 2013; Zhang et al. 2016) and the absence of complex absorption profiles (Patat et al. 2013) towards SN 2011fe suggest negligible extinction from its host galaxy. Hence, with the wide wavelength and comprehensive phase coverage dataset, the nearby, reddening-free SN 2011fe provides an excellent calibration for extinction comparison.

Assuming that SN 2012cu has the same SED as the lightly reddened SN 2011fe, the color excess curves of SN 2012cu can be directly derived by comparing the spectra of SN 2012cu with the SED templates of SN 2011fe at similar epochs (A15), as

$$E(\lambda - V)_p = -2.5[\log(\frac{f(\lambda; p)}{S_0(\lambda; p)}) - \log(\frac{f(V; p)}{S_0(V; p)})], \quad (3)$$

where at wavelength λ for phase p , $f(\lambda; p)$ and $S_0(\lambda; p)$ are flux densities from the spectra of SN 2012cu and the SED templates of SN 2011fe, respectively. Figure 1 shows the color excess curves derived from the spectroscopic data. These color excess curves are smoothed by a simple moving average method. The substantially fluctuant parts of curves beyond wavenumber $\geq 2.6\mu m^{-1}$ are also excluded.

3. Dust Models

We adopt a two-component grain model consisting of astronomical silicate and graphite (GRA, Draine & Lee 1984) or amorphous carbon (AMC, Rouleau & Martin 1991). We assume that both the silicate and carbonaceous grains have the same size distribution, i.e., a power-law function with

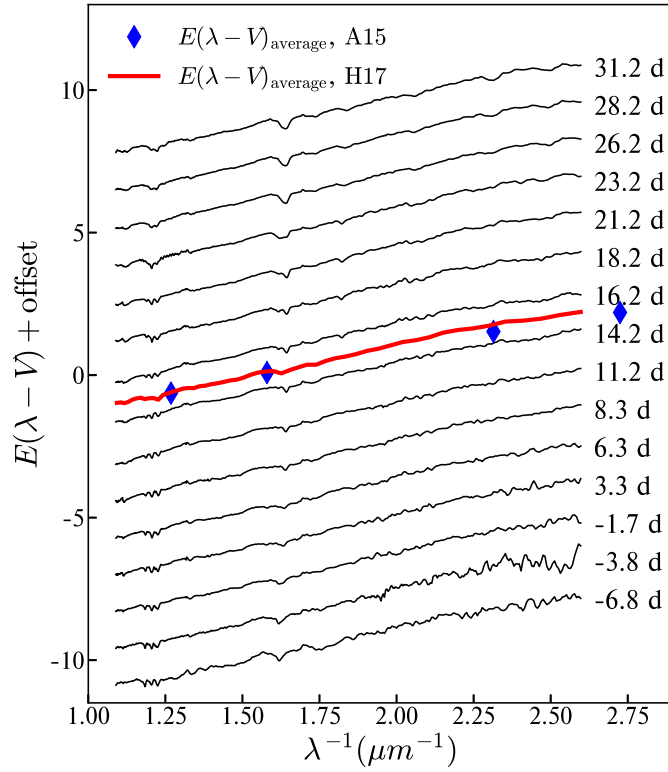


Figure 1: The derived color excess curves from the observed spectra of SN 2012cu. Black solid lines are the color excess curves of 15 epochs obtained from spectra. For comparison, the phase-averaged color excess curve is plotted in red solid line and the phase-averaged color excesses from photometric data at corresponding wavelength are shown in blue diamonds.

an exponential cutoff (Kim et al. 1994; Wang et al. 2014; Gao et al. 2015):

$$\frac{dn_i}{da} = B_i n_{\text{H}} a^{-\alpha} \exp(-a/a_b), \quad (4)$$

where α and a_b are the power index and exponential cutoff radius, respectively; dn_i is the number density of dust species i (silicate or carbonaceous component) with radii between $[a, a + da]$; n_{H} is the number density in unit of hydrogen nucleon H; B_i is the normalization constant. A classical MRN grain model (Mathis et al. 1977, hereafter MRN) has a power-law size distribution, i.e., $dn(a)/da \propto a^{-3.5}$ (Clayton et al. 2003). When $a_b \gg a$, the exponential cutoff will have $\exp(-a/a_b) \approx 1$, which decays Equation (4) to the MRN size distribution.

Based on the equations in Wang et al. (2014) (see Section 3 therein), the factor B_i can be derived from

$$B_{\text{sil}} = 1/(\rho_{\text{sil}} \int da (4\pi/3) a^3 a^{-\alpha} \exp(-a/a_b)), \quad (5)$$

for silicate dust, and

$$B_{\text{car}} = f_{\text{cs}}/(\rho_{\text{car}} \int da (4\pi/3) a^3 a^{-\alpha} \exp(-a/a_b)), \quad (6)$$

for carbonaceous dust (i.e., graphite or amorphous carbon), where f_{cs} is the mass ratio of carbonaceous dust to silicate dust, i.e., $m_{\text{car}}/m_{\text{sil}}$. The mass densities of amorphous silicate (ρ_{sil}) and graphite (ρ_{GRA}) are the same as those used in Weingartner & Draine (2001, hereafter WD01), i.e., 3.5 g cm^{-3} and 2.24 g cm^{-3} , respectively. The density of amorphous carbon (ρ_{AMC}) is 1.8 g cm^{-3} (Draine 2011).

Detailed information on the abundance of dust grains in the host galaxy of SN 2012cu remains uncertain. Therefore, we adopt three typical values of

$f_{\text{cs}} = 0, 0.3$, and 0.6 . When $f_{\text{cs}} = 0$, it means that there are no carbonaceous grains in the dust model. By assuming that the interstellar abundances in NGC 4772 are similar to those of the MW and adopting the abundance values of [Asplund et al. \(2009\)](#), the other two values of f_{cs} are derived. The value of f_{cs} will be 0.6 when the elements of Fe, Mg and Si are all in solid phase and constrained in the silicate dust, and the fraction of gas-phase carbon is 0% ([Gao et al. 2013, 2015](#); [Wang et al. 2014](#)). In addition, f_{cs} will be 0.3 when the fraction of gas-phase carbon is 50% .

Then the modeled extinction A_λ at wavelength λ is calculated by

$$A_\lambda = 1.086 N_{\text{H}} \sum_i \int_{a_{\text{min}}}^{a_{\text{max}}} da \frac{1}{n_{\text{H}}} \frac{dn_i}{da} C_{\text{ext},i}(a, \lambda), \quad (7)$$

where N_{H} and n_{H} are the column density and volume density in unit of hydrogen nucleon H, respectively. All dust grains are assumed to be spherical with the radius of $0.005 \mu\text{m} = a_{\text{min}} \leq a \leq a_{\text{max}} = 5 \mu\text{m}$. The extinction cross section $C_{\text{ext},i}(a, \lambda)$ (cm^{-2}), for the grain of species i with size a at wavelength λ , is calculated with the Mie theory code derived from BH-MIE ([Bohren & Huffman 1983](#)). The optical constants of dust are taken from [Draine & Lee \(1984\)](#) for astronomical silicate and graphite, and from [Rouleau & Martin \(1991\)](#) for amorphous carbon.

The modeled extinction $A_{X,p}$ in X band for phase p is subsequently derived from the similar formula by [A15](#):

$$A_{X,p} = -2.5 \log \left[\frac{\int T_X(\lambda) \times 10^{-0.4 \times A_\lambda} \times S_0(\lambda; p) \lambda d\lambda}{\int T_X(\lambda) \times S_0(\lambda; p) \lambda d\lambda} \right], \quad (8)$$

where the extinction A_λ is initially calculated by Equation (7); $T_X(\lambda)$ is the filter transmission, and $S_0(\lambda; p)$ is the unreddened flux density of the SED at wavelength λ for phase p (see Equation (3)).

In order to reproduce the observed extinction curves with dust models, the Levenberg-Marquardt method is generally used to perform a grid-search by minimizing χ^2 with the weights (WD01; Wang et al. 2014; A15; Nozawa 2016). Fritz et al. (2011) used $\chi^2/\text{d.o.f}$ to evaluate the goodness of fitting their observed extinction curve towards the Galactic center with different dust models. Therefore, the goodness of our fitting is evaluated by minimizing

$$\chi^2/\text{d.o.f} = \frac{1}{(N_{\text{data}} - N_{\text{para}})} \sum_{\lambda} \sum_p \frac{[E(\lambda - V)_p^{\text{mod}} - E(\lambda - V)_p^{\text{data}}]^2}{\sigma^2}, \quad (9)$$

where at wavelength λ for phase p , the modeled color excesses $E(\lambda - V)_p^{\text{mod}} \equiv A_{\lambda,p}^{\text{mod}} - A_{V,p}^{\text{mod}}$ ⁷; $E(\lambda - V)_p^{\text{data}}$ is derived from the observed data by Equation (2) and (3), for the photometric data and the spectroscopic data, respectively; $1/\sigma^2$ is the weight, i.e., the uncertainties of data; N_{data} is the number of observed data points used for fitting, and N_{para} is the number of adjustable parameters; $\text{d.o.f} \equiv N_{\text{data}} - N_{\text{para}}$ is the degree of freedom. Since we assume that the silicate and carbonaceous grains have the same dust size distribution, there are three parameters ($N_{\text{para}} = 3$) in our dust models: the size distribution power index α , the exponential cutoff size a_b , and the H column density N_{H} . The grid of α ranges from 0.4 to 5.0 with a step of 0.1, while a_b ranges from 0.01 to 0.30 with a step of 0.01.

⁷ $A_{\lambda,p}^{\text{mod}}$ is calculated by Equation (8) when fitting the photometric data, instead, by Equation (7) when fitting the spectroscopic data.

Table 1: The Results of the Best-fit Dust Models

Carbon ^a	f_{cs} ^b	α	a_b	N_{H}	$\chi^2/\text{d.o.f}$ ^c	$E(B - V)^{\text{mod}}$	A_V	A_{Ks}	R_V
			(μm)	($\times 10^{22} \text{ cm}^{-2}$)		(mag)	(mag)	(mag)	
	0	0.5	0.04	1.10	0.30	1.00	2.31	0.08	2.32
AMC	0.3	0.9	0.04	0.68	0.33	0.96	2.58	0.14	2.68
	0.6	1.2	0.04	0.49	0.34	0.96	2.59	0.16	2.69
GRA	0.3	0.5	0.03	0.68	0.33	0.97	2.67	0.17	2.75
	0.6	1.0	0.03	0.47	0.33	0.96	2.73	0.19	2.84

^a Two types of carbonaceous dust are considered in the dust model, as described in §4. AMC is amorphous carbon, and GRA is graphite.

^b f_{cs} is the mass ratio of carbonaceous dust to silicate dust, i.e., $m_{\text{car}}/m_{\text{sil}}$.

^c The values of $\chi^2/\text{d.o.f}$ are calculated with weights by considering the uncertainties (σ).

4. Results

In this work, we calculate the color excesses, $E(X - V)$ of SN 2012cu in the UV-to-NIR bands (2346–21295Å, see §2) and the color excess curves, $E(\lambda - V)$ in the optical band (3850–9150Å). We fit the combination of the color excesses and the color excess curves using the silicate+graphite/amorphous carbon dust models. The color excesses derived from the photometric data contain 31 points and cover eight epochs (i.e., $N_{\text{data}} = 31$ and phase $p = 8$). The color excess curves derived from the spectroscopic data cover 15 epochs ($p = 15$, see black lines in Figure 1). When fitting with the dust models, each of these 15 color excess curves is evenly divided into 54 points with a step of 100Å, which yields 810 points ($N_{\text{data}} = 810$) in total. Thus, in Equation (9), we finally take $p = 23$ and $N_{\text{data}} = 841$ for summation and search for the

best fitting parameters by minimizing $\chi^2/\text{d.o.f.}$

The best-fit results to our dust models are shown in Table 1. The five rows present the dust models with different types of carbonaceous component (GRA or AMC) and mass ratio f_{cs} between carbonaceous and silicate dust. In Table 1, it is clear that the modeled A_V varies from 2.31 to 2.73 mag, $E(B - V)$ ranges from 0.96 to 1.00 mag, and R_V changes from 2.32 to 2.84. The average values of A_V , $E(B - V)$, and R_V are approximately 2.6 mag, 0.97 mag, and 2.7, respectively, consistent with those of A15 and H17, i.e., $E(B - V) = 0.98 \sim 1.00$ mag and $R_V = 2.8 \sim 3.0$.

Figure 2 shows all of the five best-fit results in terms of $E(\lambda - V)$ with λ^{-1} . Blue diamonds show the color excesses derived from the photometric data, and black solid lines present the color excess curves derived from all the spectra (see black solid lines in Figure 1). Our modeled color excess curves are plotted in red solid lines. The F99 extinction curve of $R_V = 2.8$ is also shown by green dashed line for comparison. In Figure 2, all modeled color excess curves indicate that the extinction law of SN 2012cu seems much flatter in the UV bands than the F99 law of $R_V = 2.8$ with a strong 2175Å bump. By adjusting parameters (e.g., dust size distribution) of the dust models, the modeled color excess curves are feasible to display the flatness towards the UV bands even when $R_V = 2.8$. Figure 2a presents the reproduced color excess curve with no carbonaceous dust in the dust model, which yields the smallest value of $\chi^2/\text{d.o.f.}$ Because small graphite grains are usually considered as the candidate carrier of the 2175Å bump (WD01), the modeled color excess curves with GRA (Figure 2d and 2e) show weak 2175Å features and exhibit conspicuous deviations from the observed color excesses of SN 2012cu in the

UV bands, e.g., in $F225W$ and $F275W$ passbands. By contrast, the modeled color excess curves with AMC (Figure 2b and 2c) coincide with the observed data in these two passbands.

Figure 3 shows the modeled color excess curves as functions of wavelength λ . These curves extend to the mid-infrared (MIR) bands and display two absorption features [see the inset in Figure 3a] around $9.7 \mu\text{m}$ and $18 \mu\text{m}$ due to amorphous silicate (Li & Draine 2001). The profiles of these two silicate features and the corresponding mass ratio of the silicate dust cannot be further verified due to the lack of observations of SN 2012cu in MIR bandpasses.

Although our dust model presented by Figure 2a and 3a provides the minimum value of $\chi^2/\text{d.o.f}$, it still produces discernable residuals in the NIR. In addition, since the detailed abundance of NGC 4772 is not clear, we cannot simply eliminate the existence of carbonaceous dust in this host galaxy of SN 2012cu. In NGC 4772, Ciesla et al. (2014) derived the mass fraction of polycyclic aromatic hydrocarbons (PAHs) $\approx 3.25\%$ based on the dust model discussed in Draine & Li (2007), even though there is no positive evidence for the presence of PAHs features. Therefore, the dust models including AMC or GRA grains should be more reasonable compared to the $f_{\text{cs}} = 0$ case. In Figure 4 and 5, we present the normalized color excess curves in terms of $E(\lambda - V)/E(B - V)$ and the corresponding dust size distributions derived from those models with $f_{\text{cs}}^{\text{AMC}} = 0.3$ and $f_{\text{cs}}^{\text{GRA}} = 0.3$, respectively.

We also adopt the MRN size distribution to fit the color excess curves. However, the typical values of $\chi^2/\text{d.o.f}$ give 0.5 to 0.6, almost twice as the corresponding values given by our silicate+graphite/amorphous carbon dust

model shown in Table 1. Moreover, the MRN size distribution has even larger d.o.f than that of the power-law function with an exponential cutoff (Kim et al. 1994), due to the number of adjustable parameters $N_{\text{para}} = 2$, i.e., the power index α and H column density N_{H} . Therefore, we suggest that

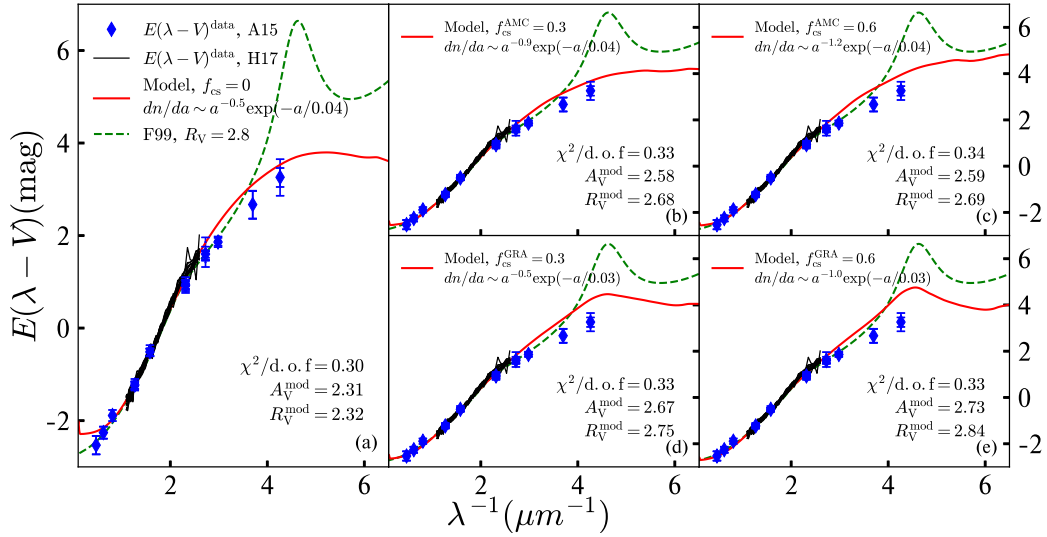


Figure 2: The modeled $E(\lambda - V)$ of SN 2012cu with λ^{-1} . Blue diamonds present the color excesses directly obtained from photometric data, and black solid lines give color excess curves derived from spectroscopic data. Red solid lines show the modeled color excess curves presented in Table 1. Panel (a) on the left provides the result with $f_{\text{cs}} = 0$. The panels in the middle (b,d) and the right (c,d) columns present the results with $f_{\text{cs}} = 0.3$ and 0.6 , respectively. The results for amorphous carbon (AMC) are shown in the upper middle (b) and the upper right (c) panels, and the results for graphite (GRA) are presented in the lower middle (d) and the lower right (e) panels. For comparison, in each panel, we overplot the F99 extinction curves of $R_V = 2.8$ in green dashed line.

Table 2: The Dust Extinction towards SN 2012cu

Band	λ (μm)	$f_{\text{cs}}^{\text{AMC}} = 0.3^{\text{a}}$		$f_{\text{cs}}^{\text{GRA}} = 0.3^{\text{b}}$	
		A_{λ} (mag)	C_{ext}/H (cm^2/H)	A_{λ} (mag)	C_{ext}/H (cm^2/H)
Ly edge	0.091	6.55	9.67×10^{-22}	7.06	1.04×10^{-21}
Ly α	0.122	6.64	9.80×10^{-22}	7.07	1.04×10^{-21}
UVW2/UVOT	0.203	6.61	9.76×10^{-22}	7.04	1.03×10^{-21}
UVM2/UVOT	0.223	6.42	9.48×10^{-22}	7.10	1.04×10^{-21}
UVW1/UVOT	0.259	5.90	8.71×10^{-22}	6.31	9.25×10^{-22}
F225W/HST	0.287	5.52	8.15×10^{-22}	5.74	8.42×10^{-22}
F275W/HST	0.290	5.47	8.09×10^{-22}	5.70	8.34×10^{-22}
F218W/HST	0.311	5.17	7.64×10^{-22}	5.33	7.82×10^{-22}
F336W/HST	0.340	4.74	7.01×10^{-22}	4.88	7.15×10^{-22}
u/SDSS	0.355	4.54	6.71×10^{-22}	4.66	6.83×10^{-22}
U	0.365	4.41	6.51×10^{-22}	4.52	6.63×10^{-22}
F438W/HST	0.433	3.61	5.33×10^{-22}	3.71	5.44×10^{-22}
B	0.440	3.54	5.23×10^{-22}	3.64	5.34×10^{-22}
F467M/HST	0.468	3.26	4.82×10^{-22}	3.36	4.93×10^{-22}
g/SDSS	0.469	3.26	4.81×10^{-22}	3.36	4.92×10^{-22}
V	0.550	2.58	3.81×10^{-22}	2.67	3.91×10^{-22}
F555W/HST	0.550	2.58	3.81×10^{-22}	2.67	3.91×10^{-22}
r/SDSS	0.617	2.14	3.15×10^{-22}	2.23	3.27×10^{-22}
F631N/HST	0.630	2.06	3.04×10^{-22}	2.16	3.16×10^{-22}
R	0.700	1.70	2.51×10^{-22}	1.80	2.64×10^{-22}
i/SDSS	0.748	1.50	2.21×10^{-22}	1.60	2.35×10^{-22}
F814W/HST	0.792	1.34	1.97×10^{-22}	1.44	2.11×10^{-22}
F845M/HST	0.863	1.12	1.66×10^{-22}	1.23	1.80×10^{-22}
z/SDSS	0.893	1.05	1.55×10^{-22}	1.15	1.68×10^{-22}
I	0.900	1.03	1.52×10^{-22}	1.13	1.66×10^{-22}
J/2MASS	1.235	0.51	7.51×10^{-23}	0.58	8.57×10^{-23}
H/2MASS	1.662	0.25	3.76×10^{-23}	0.30	4.45×10^{-23}
K _s /2MASS	2.159	0.14	2.10×10^{-23}	0.17	2.52×10^{-23}
W1/WISE	3.353	0.07	1.00×10^{-23}	0.07	1.07×10^{-23}
L	3.450	0.07	9.65×10^{-24}	0.07	1.02×10^{-23}
[3.6]/IRAC	3.545	0.06	9.31×10^{-24}	0.07	9.72×10^{-24}
[4.5]/IRAC	4.442	0.05	6.80×10^{-24}	0.05	6.70×10^{-24}
W2/WISE	4.603	0.04	6.48×10^{-24}	0.04	6.35×10^{-24}
M	4.800	0.04	6.15×10^{-24}	0.04	5.98×10^{-24}
[5.8]/IRAC	5.675	0.04	5.31×10^{-24}	0.03	4.95×10^{-24}
[8.0]/IRAC	7.760	0.05	7.31×10^{-24}	0.04	6.43×10^{-24}
N	10.600	0.15	2.21×10^{-23}	0.15	2.15×10^{-23}
W3/WISE	11.561	0.10	1.53×10^{-23}	0.10	1.47×10^{-23}
Q	21.000	0.06	8.55×10^{-24}	0.06	8.72×10^{-24}
W4/WISE	22.088	0.05	7.62×10^{-24}	0.05	7.85×10^{-24}

^a The silicate+amorphous carbon dust model with $f_{\text{cs}}^{\text{AMC}} = 0.3$.

^b The silicate+graphite dust model with $f_{\text{cs}}^{\text{GRA}} = 0.3$.

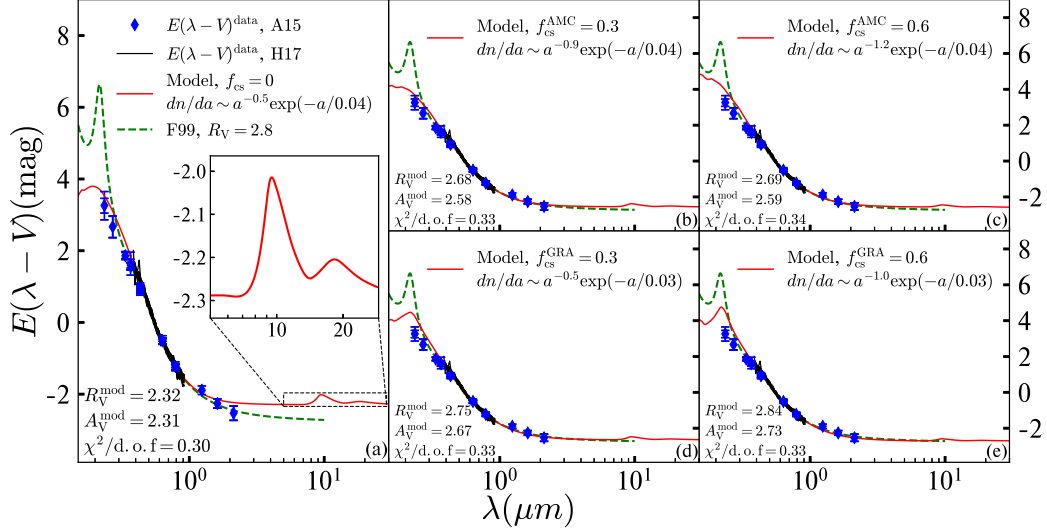


Figure 3: Same as Figure 2, but for the modeled $E(\lambda - V)$ with λ . The inset in panel (a) shows the detailed fitting curve in the MIR bands.

5. Discussion: The Extinction Law and dust properties towards SN 2012cu

Since the existence of carbonaceous dust in NGC 4772 cannot be simply eliminated (see §4), Figure 4 shows two best-fit results in terms of $E(\lambda - V)/E(B - V)$ when $f_{\text{cs}} \neq 0$, in comparison with the extinction curves calculated with the F99 law of $R_V = 2.8$, the average MW extinction curve of $R_V = 3.1$, the extinction curve of the SMC bar (WD01), the Calzetti attenuation law (Calzetti et al. 1994) for starburst galaxies, and the mean extinction curve of five mostly reddened individual AGNs (Gaskell & Benker 2007)⁸. With the silicate+graphite model ($f_{\text{cs}}^{\text{GRA}} = 0.3$), the modeled ex-

⁸Gaskell & Benker (2007) derived average extinction curves of five mostly reddened AGNs in their sample, and they found that these curves extend flatly towards the far-UV

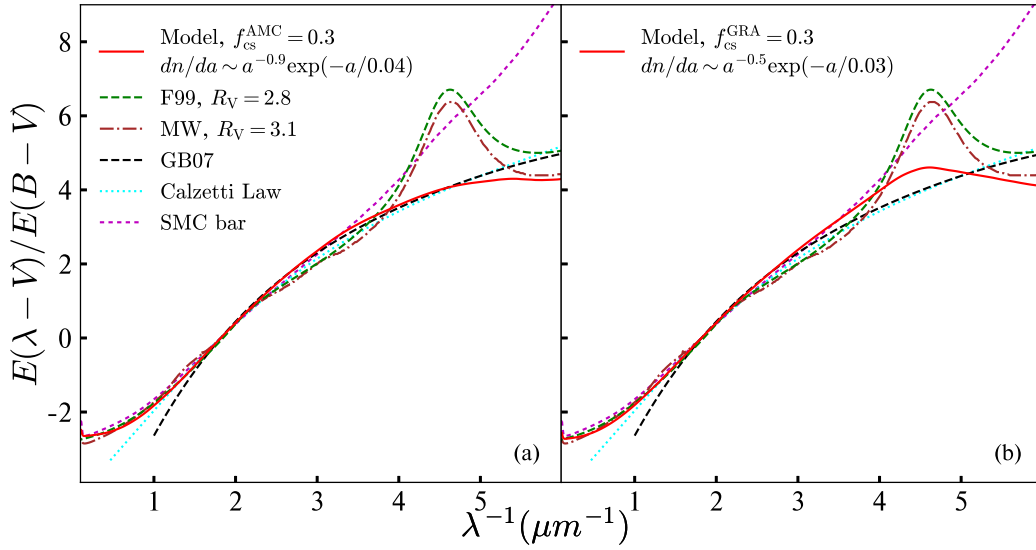


Figure 4: Comparison of the normalized color excess curves $E(\lambda-V)/E(B-V)$ towards SN 2012cu derived from silicate+amorphous carbon dust model ($f_{\text{cs}}^{\text{AMC}} = 0.3$) [Panel (a)] and silicate+graphite dust model ($f_{\text{cs}}^{\text{GRA}} = 0.3$) [Panel (b)]. Our modeled curves are denoted with red solid lines, while the F99 extinction laws of $R_V = 2.8$ and $R_V = 3.1$ (MW average) are denoted with green dashed lines and brown dot-dashed lines, respectively. We also show the extinction curve of the SMC bar (magenta short dashed line), the mean reddening curve of AGNs (black dashed line, [Gaskell & Benker 2007](#)), and the Calzetti attenuation law for starburst galaxies (cyan dotted line, [Calzetti et al. 1994](#)).

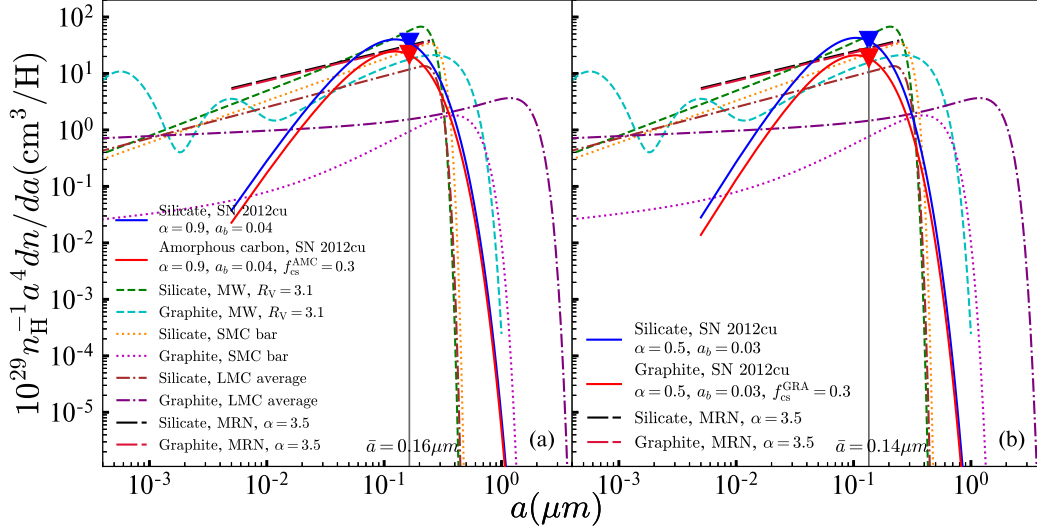


Figure 5: Size distributions of silicate+amorphous carbon dust model (a) and silicate+graphite dust model (b) when $f_{\text{cs}} = 0.3$. The size distributions of silicate and carbonaceous dust are denoted with blue and red solid lines, respectively. The triangles on these lines represent the average sizes derived from the curves. For comparison, the WD01 (Weingartner & Draine 2001) size distributions of silicate and graphite for the average Galactic extinction law of $R_V = 3.1$ (green and cyan dashed lines), for the SMC (orange and magenta dotted lines), and for the LMC (brown and purple dot-dashed lines) are overplotted, respectively. The MRN size distribution with $\alpha = 3.5$ (Draine & Lee 1984) is also shown by long dashed lines (crimson for silicate and black for graphite).

tion curves exhibit the 2175Å bump produced by small graphite dust and display discernable deviation from the observed curve in the UV bands. On the contrary, the silicate+amorphous carbon model ($f_{\text{cs}}^{\text{AMC}} = 0.3$) has no 2175Å feature and it well reproduces the extinction curve in *F225W* and *F275W* passbands.

In Figure 4a, the modeled extinction curves are much flatter in the UV bands than those of the MW and the SMC bar. It suggests that the size of the dust in the ISM towards SN 2012cu in NGC 4772 tends to be larger than that of the MW, and even much larger than that of the SMC bar. Our modeled extinction curves in the UV bands are nearly similar with the mean reddening curve of AGNs (Gaskell & Benker 2007)⁹.

A15 used all measured colors (UV-NIR) to derive the extinction curves of SN 2012cu with F99 extinction law. Their best-fit result suggests $R_V = 2.8 \pm 0.1$, which is shown by green dashed line in Figure 4. H17 similarly utilized F99 law to deredden SN 2012cu spectra with the best fitting parameters $E(X - V) = 1.0$ mag and $R_V = 2.95$. The extinction curves and R_V of SN 2012cu derived in this work are, however, based on the detailed dust models for the observed color excesses. The best-fit values of R_V for all the cases listed in Table 1 are generally consistent with the studies by A15 and H17. In Figure 4b, the presence of a weak 2175Å bump suggests the existence of

bands without the 2175Å bump. Calzetti et al. (1994) derived the attenuation curves of starburst galaxies, which similarly show the flattening and no appreciable 2175Å bump.

⁹Li (2007) compared the AGN's extinction curves derived from composite quasar spectra by Czerny et al. (2004) and Gaskell et al. (2004) with the mean extinction curve of AGNs by Gaskell & Benker (2007) (see Li 2007 and Figure 3 therein).

graphite as the carbonaceous component merged in the dust model. Although the F99 law of $R_V = 2.8$ also presents the 2175Å feature, the profile is too strong to reproduce the flattening of the UV extinction curve with the same value of R_V .

Figure 5 shows the derived size distributions of silicate and carbonaceous dust when $f_{cs} = 0.3$, in comparison with a variety of interstellar dust size distributions. The average radii of two types of dust grains are presented as $0.16 \mu\text{m}$ in Figure 5a and $0.14 \mu\text{m}$ in Figure 5b, respectively. For the average extinction law of the MW dust with $R_V = 3.1$, Nozawa (2016) presented the average size $\bar{a} \sim 0.01 \mu\text{m}$ with the dust model consisting of silicate and graphite¹⁰. Compared to Nozawa (2016), the average sizes of dust grains derived in our study are larger by approximately a factor of 10. According to the modeled extinction laws of SN 2012cu in Figure 4, we therefore infer that the size distribution of NGC 4772 is biased to large sizes compared with those of the MW, the LMC and the SMC.

In Table 2, we present the modeled extinction correction A_λ towards SN 2012cu in NGC 4772 with the dust models with $f_{cs}^{\text{AMC}} = 0.3$ and $f_{cs}^{\text{GRA}} = 0.3$. These modeled extinction corrections cover most of the commonly used astronomical filters.

¹⁰Nozawa (2016) calculated the average radii weighted by the size distribution of dust [see Equation (8) therein], for distinguishing the similarity between an exponential-like distribution and a lognormal distribution. We adopt the same equation to derive the average radii for comparing the typical sizes of dust grains in the MW. Note that the extinction law depends more probably on the size distribution of dust rather than average radii of dust grains.

6. Conclusion

In this work, we use the broadband photometric data provided by A15 and optical spectroscopic data obtained from H17 to study the extinction of SN 2012cu. We adopt silicate+graphite/amorphous carbon dust models to fit the observed color excess curves of SN 2012cu and derive the extinction as a function of wavelength (i.e., A_λ).

The best-fit results give the visual extinction towards SN 2012cu of $A_V \approx 2.6$ mag, the reddening of $E(B - V) \approx 1.0$ mag, and the total-to-selective extinction ratio $R_V \approx 2.7$. The reasonable modeled A_λ towards SN 2012cu in NGC 4772 are also presented in Table 2 for extinction corrections. The modeled extinction curves towards the SN 2012cu sightline extend flatly to the far-UV bands with or without a very weak 2175Å feature, and are much flatter than those of the MW, the LMC, and the SMC. The flatness of the UV extinction curves suggests a “grey” line-of-sight extinction law towards the host AGN galaxy of NGC 4772, and indicates that the size distribution of dust in this sightline is skewed to large grains. The extragalactic extinction laws are inadequately based on R_V and probably dependent on the local interstellar environment.

Acknowledgements

We acknowledge Amanullah, R. for providing the SED templates of SN 2011fe. We thank Prof. Li, A., Dr. Nozawa, T., and the anonymous referees for their very helpful suggestions/comments. We are grateful to the helpful discussion during the 10th ‘Cosmic Dust’ conference held by NAOJ. This work is supported by NSFC Projects U1631104, and 11533002.

References

- Amanullah, R., et al., 2014, The Peculiar Extinction Law of SN 2014J Measured with the Hubble Space Telescope, *Astrophys. J.*, 788, L21 (6pp).
- Amanullah, R., et al., 2015, Diversity in extinction laws of Type Ia supernovae measured between 0.2 and 2 μm , *Mon. Not. R. Astron. Soc.*, 453, 3300-3328. (A15)
- Asplund, M., Grevesse, N., Sauval, A. J., Scott, P., 2009, The Chemical Composition of the Sun, *Annu. Rev. Astronom. Astrophys.*, 47, 481-522.
- Bohren, C. F., Huffman, D. R., 1983, Absorption and scattering of light by small particles, *New York: Wiley*.
- Brown, P. J., et al., 2015, Swift Ultraviolet Observations of Supernova 2014J in M82: Large Extinction from Interstellar Dust, *Astrophys. J.*, 805, 74 (13pp).
- Buton, C., et al., 2013, Atmospheric extinction properties above Mauna Kea from the Nearby SuperNova Factory spectro-photometric data set, *Astronom. Astrophys.*, 549, A8 (21pp).
- Calzetti, D., Kinney, A. L., Storchi-Bergmann, T., 1994, Dust extinction of the stellar continua in starburst galaxies: The ultraviolet and optical extinction law, *Astrophys. J.*, 429, 582-601.
- Cardelli, J. A., Clayton, G. C., Mathis, J. S., 1989, The relationship between infrared, optical, and ultraviolet extinction, *Astrophys. J.*, 345, 245-256. (CCM89)

- Ciesla, L., et al., 2014, Dust spectral energy distributions of nearby galaxies: an insight from the Herschel Reference Survey, [Astronom. Astrophys.](#), 565, A128 (33pp).
- Cikota, A., Deustua, S., Marleau, F., 2016, Determining Type Ia Supernova Host Galaxy Extinction Probabilities and a Statistical Approach to Estimating the Absorption-to-reddening Ratio R_V , [Astrophys. J.](#), 819, 152 (13pp).
- Clayton, G. C., et al., 2003, Dust Grain Size Distributions from MRN to MEM, [Astrophys. J.](#), 588, 871-880.
- Czerny, B., Li, J., Loska, Z., Szczerba, R., 2004, Extinction due to amorphous carbon grains in red quasars from the Sloan Digital Sky Survey, [Mon. Not. R. Astron. Soc.](#), 348, L54-L57.
- Djupvik, A. A., Andersen, J., 2010, The Nordic Optical Telescope, [Astrophys. Space Sci. Proc.](#), 14, 211.
- Draine, B. T., 2011, Physics of the Interstellar and Intergalactic Medium, [Princeton University Press](#), ISBN: 978-0-691-12214-4.
- Draine, B. T., Lee, H. M., 1984, Optical properties of interstellar graphite and silicate grains, [Astrophys. J.](#), 285, 89-108.
- Draine, B. T., Li, A., 2007, Infrared Emission from Interstellar Dust. IV. The Silicate-Graphite-PAH Model in the Post-Spitzer Era, [Astrophys. J.](#), 657, 810-837.

- Fitzpatrick, E. L., 1999, Correcting for the Effects of Interstellar Extinction, [Publ. Astronom. Soc. Paci.](#), 111, 63-75. (F99)
- Fitzpatrick, E. L., & Massa, D., 2007, An Analysis of the Shapes of Interstellar Extinction Curves. V. The IR-through-UV Curve Morphology, [Astrophys. J.](#), 663, 320-341.
- Folatelli, G., et al., 2010, The Carnegie Supernova Project: Analysis of the First Sample of Low-Redshift Type-Ia Supernovae, [Astronom. J.](#), 139, 120-144.
- Foley, R. J., et al., 2014, Extensive HST ultraviolet spectra and multiwavelength observations of SN 2014J in M82 indicate reddening and circumstellar scattering by typical dust, [Mon. Not. R. Astron. Soc.](#), 443, 2887-2906.
- Fritz, T. K., et al., 2011, Line Derived Infrared Extinction toward the Galactic Center, [Astrophys. J.](#), 737, 73 (21pp).
- Gao, J., et al., 2015, Physical Dust Models for the Extinction toward Supernova 2014J in M82, [Astrophys. J.](#), 807, L26 (6pp).
- Gao, J., Li, A., Jiang, B. W., 2013, Modeling the infrared extinction toward the galactic center, [Earth Planets Space](#), 65, 1127-1132.
- Gaskell, C. M., Benker, A. J., 2007, AGN Reddening and Ultraviolet Extinction Curves from Hubble Space Telescope Spectra, [arXiv:0711.1013](#).
- Gaskell, C. M., Goosmann, R. W., Antonucci, R. R. J., Whysong, D. H., 2004, The Nuclear Reddening Curve for Active Galactic Nuclei

- and the Shape of the Infrared to X-Ray Spectral Energy Distribution, [Astrophys. J.](#), 616, 147-156.
- Goobar, A., 2008, Low R_V from Circumstellar Dust around Supernovae, [Astrophys. J.](#), 686, L103-L106.
- Goobar, A., et al., 2014, The Rise of SN 2014J in the Nearby Galaxy M82, [Astrophys. J.](#), 784, L12 (6pp).
- Gordon, K. D., et al., 2003, A Quantitative Comparison of the Small Magellanic Cloud, Large Magellanic Cloud, and Milky Way Ultraviolet to Near-Infrared Extinction Curves, [Astrophys. J.](#), 594, 279-293.
- Hamuy, M., Phillips, M. M., Wells, L. A., Maza, J., 1993, K Corrections for type IA supernovae, [Publ. Astronom. Soc. Paci.](#), 105, 787-793.
- Haynes, M. P., et al., 2000, Kinematic Evidence of Minor Mergers in Normal SA Galaxies: NGC 3626, NGC 3900, NGC 4772, and NGC 5854, [Astronom. J.](#), 120, 703-727.
- Ho, L. C., Filippenko, A. V., Sargent, W. L. W., Peng, C. Y., 1997, A Search for “Dwarf” Seyfert Nuclei. IV. Nuclei with Broad $H\alpha$ Emission, [Astrophys. J. Suppl.](#), 112, 391-414.
- Huang, X., et al., 2017, The Extinction Properties of and Distance to the Highly Reddened Type IA Supernova 2012CU, [Astrophys. J.](#), 836, 157 (18pp). (H17)
- Itagaki, K., et al., 2012, Supernova 2012cu in NGC 4772 = Psn J12532935+0209390, [Central Bureau Electronic Telegrams](#), 3146, 1.

- Kim, S.-H., Martin, P. G., Hendry, P. D., 1994, The size distribution of interstellar dust particles as determined from extinction, [Astrophys. J.](#), 422, 164-175.
- Li, A., 2007, Dust in Active Galactic Nuclei, [ASP Conf. Ser.](#), 373, 561–572.
- Li, A., Draine, B. T., 2001, Infrared Emission from Interstellar Dust. II. The Diffuse Interstellar Medium, [Astrophys. J.](#), 554, 778-802.
- Marion, G. H., Milisavljevic, D., Rines, K., Wilhelmy, S., 2012, Supernova 2012cu in NGC 4772 = PSN J12532935+0209390., [Central Bureau Electronic Telegrams](#), 3146, 2.
- Mathis, J. S., Rumpl, W., Nordsieck, K. H., 1977, The size distribution of interstellar grains, [Astrophys. J.](#), 217, 425-433. (MRN)
- Mazzali, P. A., et al., 2014, Hubble Space Telescope spectra of the Type Ia supernova SN 2011fe: a tail of low-density, high-velocity material with $Z < Z_{\odot}$, [Mon. Not. R. Astron. Soc.](#), 439, 1959-1979.
- Nobili, S., Goobar, A., 2008, The colour-lightcurve shape relation of type Ia supernovae and the reddening law, [Astronom. Astrophys.](#), 487, 19-31.
- Nozawa, T., 2016, Properties of interstellar dust responsible for extinction laws with unusually low total-to-selective extinction ratios of $R_V=1-2$, [Planet. Space Sci.](#), 133, 36-46.
- Nugent, P. E., et al., 2011, Supernova SN 2011fe from an exploding carbon-oxygen white dwarf star, [Nat.](#), 480, 344-347.

- Patat, F., et al., 2007, Detection of Circumstellar Material in a Normal Type Ia Supernova, [Sci.](#), 317, 924-926.
- Patat, F., et al., 2013, Multi-epoch high-resolution spectroscopy of SN 2011fe. Linking the progenitor to its environment, [Astronom. Astrophys.](#), 549, A62 (10pp).
- Pereira, R., et al., 2013, Spectrophotometric time series of SN 2011fe from the Nearby Supernova Factory, [Astronom. Astrophys.](#), 554, A27 (22pp).
- Perlmutter, S., et al., 1999, Measurements of Ω and Λ from 42 High-Redshift Supernovae, [Astrophys. J.](#), 517, 565-586.
- Riess, A. G., et al., 1998, Observational Evidence from Supernovae for an Accelerating Universe and a Cosmological Constant, [Astronom. J.](#), 116, 1009-1038.
- Riess, A. G., et al., 2016, A 2.4% Determination of the Local Value of the Hubble Constant, [Astrophys. J.](#), 826, 56 (31pp).
- Rouleau, F., Martin, P. G., 1991, Shape and clustering effects on the optical properties of amorphous carbon, [Astrophys. J.](#), 377, 526-540.
- Schlafly, E. F., Finkbeiner, D. P., 2011, Measuring Reddening with Sloan Digital Sky Survey Stellar Spectra and Recalibrating SFD, [Astrophys. J.](#), 737, 103 (13pp).
- Stritzinger, et al., 2002, Optical Photometry of the Type Ia Supernova 1999ee and the Type Ib/c Supernova 1999ex in IC 5179, [Astronom. J.](#), 124, 2100-2117.

- Tully, R. B., et al., 2008, Our Peculiar Motion Away from the Local Void, [Astrophys. J.](#), 676, 184-205.
- Tully, R. B., et al., 2009, The Extragalactic Distance Database, [Astronom. J.](#), 138, 323-331.
- Wang, L., 2005, Dust around Type Ia Supernovae, [Astrophys. J.](#), 635, L33-L36.
- Wang, S., Li, A., Jiang, B. W., 2014, Modeling the infrared interstellar extinction, [Planet. Space Sci.](#), 100, 32-39.
- Weingartner, J. C., Draine, B. T., 2001, Dust Grain-Size Distributions and Extinction in the Milky Way, Large Magellanic Cloud, and Small Magellanic Cloud, [Astrophys. J.](#), 548, 296-309. (WD01)
- Yang, Y., et al., 2017, Interstellar-medium Mapping in M82 through Light Echoes around Supernova 2014J, [Astrophys. J.](#), 834, 60 (15pp).
- Zhang, K., et al., 2016, Optical Observations of the Type Ia Supernova SN2011fe in M101 for Nearly 500 Days, [Astrophys. J.](#), 820, 67 (17pp).